Electrochimica Acta 57 (2011) 277–284

Contents lists available at ScienceDirect

Electrochimica Acta

journal homepage: www.elsevier.com/locate/electacta

Conducting polymer-based counter electrode for a quantum-dot-sensitized solar cell (QDSSC) with a polysulfide electrolyte☆

Min-Hsin Yeh[a], Chuan-Pei Lee[a], Chen-Yu Chou[a], Lu-Yin Lin[a], Hung-Yu Wei[b], Chih-Wei Chu[c,d], R. Vittal[a], Kuo-Chuan Ho[a,b,*,1]

[a] Department of Chemical Engineering, National Taiwan University, Taipei 10617, Taiwan
[b] Institute of Polymer Science and Engineering, National Taiwan University, Taipei 10617, Taiwan
[c] Research Center for Applied Sciences, Academia Sinica, Taipei 11529, Taiwan
[d] Department of Photonics, National Chiao Tung University, Hsinchu 30010, Taiwan

ARTICLE INFO

Article history:
Received 30 November 2010
Received in revised form 23 March 2011
Accepted 24 March 2011
Available online 2 April 2011

Keywords:
Conducting polymers
Counter electrode
Electrochemical polymerization
Electrocatalytic activity
Quantum-dot-sensitized solar cell

ABSTRACT

Conducting polymer materials, i.e., polythiophene (PT), polypyrrole (PPy), and poly(3,4-ethylenedioxythiophene) (PEDOT) were used to prepare counter electrodes (CEs) for quantum-dot-sensitized solar cells (QDSSCs). The QDSSC with PEDOT-CE exhibited the highest solar-to-electricity conversion efficiency (η) of 1.35%, which is remarkably higher than those of the cells with PT-CE (0.09%) and PPy-CE (0.41%) and very slightly higher than that of the cell with sputtered-gold-CE (1.33%). Electrochemical impedance spectra (EIS) show that this highest conversion efficiency of the PEDOT-based cell is due to higher electrocatalytic activity and reduced charge transfer resistance at the interface of the CE and the electrolyte, compared to those in the case of the cells with other conducting polymers and bare Au. Furthermore, the influences of morphology of the PEDOT film and the charge passed for its electropolymerization on the performance of its QDSSC were also studied. The higher porosity and surface roughness of the PEDOT matrix, with reference to those of other polymers are understood to be the reason for PEDOT to possess higher electrocatalytic activity at its interface with electrolyte.

1. Introduction

Since the inception of intensive research on dye-sensitized solar cells (DSSCs) by Grätzel and his co-worker in 1991 [1], the cells have attracted a lot of attention, attributable to their low cost and relatively high energy conversion efficiency [2–6]. In a DSSC, the photosensitizing dye, adsorbed on the nanocrystalline TiO_2 film, plays an important role in determining the light absorption and subsequent electron-transfer process, and has been regarded as one of the key factors to govern the light-to-electricity conversion efficiency (η) of the cell. At present, the DSSCs with ruthenium-based dyes, such as N3 [5], N719 [2], CYC-B1 [7] and CYC-B11 [8] have shown efficiencies up to 10% and more. Recently, narrow band gap semiconductor quantum dots (QDs), such as CdS [9–13], CdSe [14–17], PbS [18], PbSe [19], InP [20], InAs [21], and ZnSe [22] have been introduced as photosensitizers for solar cells, and the pertinent cells are called quantum-dot-sensitized solar cells (QDSSCs). The distinctive characteristics of QDs over the conventional dyes are their strong photo-response in the visible region and their quantum confinement effects [21,23,24]. Moreover, QDs possess tunable optical properties and band gaps depending on the particle size (quantum size effect). Higher conversion efficiencies for QDSSCs are expected to be obtained owing to these characters. The theoretically maximum conversion efficiency of QDSSCs (44%) [25] is considerably higher than that of DSSCs (31%), according to the calculations of Shockley and Queisser [26].

Although several designs have been proposed for QDSSCs, based on the benefits of hot electrons [27] or carrier multiplication [28], the cell efficiency of the QDSSCs (around ~3%) is still lower than that of the DSSCs (more than 10%). The poor performance of QDSSCs is mainly due to narrow adsorption range of QDs, weak electron collection by the TiO_2 from the QDs [29], and due to charge recombination at the QDs–electrolyte interface [14]. In order to increase the efficiency of QDSSCs, search for novel electrocatalytic materials for their counter electrodes (CEs) is necessary. In DSSCs, platinum (Pt) is most common electrocatalytic material and is employed to facilitate the reduction of triiodide (I_3^-) ions, the redox couple in the

☆ This manuscript was presented at the 12th International Symposium on Polymer Electrolyte (ISPE-12), Symposium A-New Materials, August 29–September 3, 2010, Padova, Italy.

* Corresponding author at: Department of Chemical Engineering, National Taiwan University, Taipei 10617, Taiwan. Tel.: +886 2 2366 0739; fax: +886 2 2362 3040.
E-mail address: kcho@ntu.edu.tw (K.-C. Ho).
[1] ISE member.

0013-4686/$ – see front matter © 2011 Elsevier Ltd. All rights reserved.
doi:10.1016/j.electacta.2011.03.097

electrolyte being I^-/I_3^- ions. However, polysulfide (S_x^{2-}/S^{2-}) electrolyte is more suitable as the redox couple in the case of QDSSCs, because QDs will be degraded if I^-/I_3^- electrolyte is used as the redox couple. Besides, it has been reported that polysulfide electrolyte allows strong interactions between Pt and S^{2-}, in which the latter adsorbs onto the surface of Pt and suppresses the conductivity, electrocatalytic activity and electrochemical surface area of the CE [13]. In order to solve this problem, Pt-free CEs, such as those prepared with Au [30], carbon [31], structured carbon material [32,33], Cu_2S [16,34], and CoS [35], have been suggested by several authors for QDSSCs. On the other hand, conducting polymers became promising candidates as counter electrode materials for DSSCs, because of their advantages, e.g., low cost-availability, high conductivity, large electrochemical surface area, and good electrocatalytic activity for I_3^- reduction [36–41].

In this study, three conducting polymers, i.e., polypyrrole (PPy), polythiophene (PT), and poly(3,4-ethylenedioxythiophene) (PEDOT), prepared by electrochemical polymerization have been used as CE materials for QDSSCs; the photovoltaic performances of the cells are compared. Furthermore, the influences of morphology of PEDOT film, namely, the charge passed for its electrodeposition on the performance of a QDSSC were also studied. The performance of the QDSSC with PEDOT-CE is compared and contrasted with those of the cells with PT-CE, PPy-CE and sputtered-gold-CE (s-Au-CE). This is the first report on the use of conducting polymers as CE materials for the fabrication of QDSSCs. The efficiency achieved in this study for the QDSSC with PEDOT-CE (1.35%) is comparable to that of the cell with s-Au-CE (1.33%), both cells being sensitized by the quantum dots, CdS. The maximum efficiency for a QDSSC sensitized with CdS and with Au-CE is around 1.84% [13].

2. Experimental

2.1. Materials

Cadmium nitrate ($Cd(NO_3)_2{\cdot}4H_2O$, ≥99%), sodium sulfide ($Na_2S{\cdot}9H_2O$, ≥98%), sulfur (S), potassium chloride (KCl, ≥99%), Ti(IV) tetraisopropoxide (TTIP, ≥98%), 2-methoxyethanol (≥99.5%), ethanol (99.8%), methanol (99.8%), isopropanol (99.8%), lithium perchlorate ($LiClO_4$, ≥98.0%) and 3,4-ethylenedioxythiophene (EDOT, 97%) were obtained from Aldrich. Poly(ethylene glycol) (PEG, MW ~20,000) was obtained from Merck. Acetonitrile (99.99%) and nitric acid (ca. 65% solution in water) were obtained from J.T. Baker. Thiophene (99+%) and pyrrole (99%) were obtained from Acros. The pyrrole monomer used for this study was purified by a vacuum distillation before being used in electropolymerization.

2.2. Preparation and characterization of photoanode and conducting polymer-based counter electrode

The preparation of TiO_2 paste and the electrode fabrication were carried out based on previous literatures [42–44]. TTIP of 72 mL was added to 430 mL of 0.1 M nitric acid solution with constant stirring and the contents were heated to 88 °C for 8 h. When the mixture was cooled down to room temperature, the resultant colloid was filtered and heated in an autoclave at 240 °C for 12 h in order to allow the growth of the TiO_2 nanoparticles. The TiO_2 colloid was concentrated to 13 wt%, and 30 wt% (with respect to TiO_2) of PEG was added to it to prevent the film from cracking during drying.

Fluorine-doped SnO_2 (FTO, TEC-7, ~10 Ω sq^{-1}, NSG America, Inc., NJ, USA) and tin-doped In_2O_3 (ITO, UR-ITO007-0.7 mm, ~10 Ω sq^{-1}, Uni-onward Corp., Taipei, Taiwan) conducting glasses were first cleaned with a neutral cleaner and then washed with deionic water (DI-water), acetone, and isopropanol sequentially. The conducting surface of the FTO was treated with a solution of TTIP in 2-methoxyethanol (weight ratio = 1:3) for obtaining a good mechanical contact between the conducting glass and the TiO_2 film, as well as for isolating the conducting glass surface from the electrolyte. A 10 μm-thick film of TiO_2 was coated on the treated FTO glass by doctor blade method, and a portion of 0.4 cm × 0.4 cm was selected from it for active area by removing the side portions by scrapping. The as-prepared TiO_2 film was gradually heated to 450 °C (rate = 10 °C/min) in an oxygen atmosphere, and subsequently sintered at that temperature for 30 min.

The prepared TiO_2 electrode was dipped into 0.4 M $Cd(NO_3)_2$ in ethanol for 5 min, rinsed with pure ethanol, dried with N_2, dipped into 0.4 M Na_2S in methanol for 5 min, and then rinsed with pure methanol, dried with N_2. This procedure was termed as 1 successive ionic layer adsorption and reaction (SILAR) cycle [9]. According to the literature [49], 5 SILAR cycles of QD-photoanode rendered the best cell efficiency.

On the other hand, a conducting polymer film was obtained through electropolymerization using a bath solution consisting of 0.1 M monomer and 0.1 M $LiClO_4$ in acetonitrile, and using a three-electrode system, i.e., an ITO conducting glass as the working electrode, a Pt foil as the counter electrode and an Ag/Ag^+ reference electrode, with a potentiostat (Autolab, PGSTAT302N, Eco-Chemie, the Netherlands). Different conducting polymer films (PT, PPy, and PEDOT) were obtained by applying different potentials (1.8 V, 1.0 V and 1.1 V *vs.* Ag/Ag^+) until a charge capacity of 40 mC cm^{-2} was reached. Sputtered-gold (s-Au) and sputtered-platinum (s-Pt) electrodes were prepared by sputtering for 105 s and 240 s, respectively. The films, s-Au and s-Pt have the same thickness, i.e., 50 nm (obtained from the calibration curve of sputtering). Surface morphologies of s-Au, PT, PPy, and PEDOT films on ITO conducting glasses were observed by using scanning electron microscopy (SEM, Nova NanoSEM 230, FEI). The topographies of PEDOT and s-Au films were studied by atomic force microscopy (AFM), with a scanning probe microscope with a NanoScopes IIIa controller, operated in tapping mode, equipped with the extended electronics module, which enables height imaging in tapping mode. The range of resonance frequencies of cantilever for the film of PEDOT is 96–175 kHz (force constant: 5–37 N/m) and the resonance frequency for the film of s-Au is 320 kHz (force constant: 42 N/m) (values were obtained from the supplier).

2.3. Cell assembly and measurements

The thus prepared TiO_2/CdS photoanode was attached to the s-Au-CE or different CP-based-CEs to fabricate the cell. The two electrodes were separated by a 25 μm-thick Surlyn® (SX1170-25, Solaronix S.A., Aubonne, Switzerland) and sealed by heating. A solution consisting of Na_2S (0.5 M), S (2.0 M), KCl (0.2 M) in MeOH/water (7:3 by volume) was used as the electrolyte [30]. The prepared electrolyte was injected into the gap between the electrodes through a hole by capillarity.

The surface of the QDSSC was illuminated by a class A quality solar simulator (XES-301S, AM1.5G, San-Ei Electric), and the incident light intensity (100 mW cm^{-2}) was calibrated with a standard Si cell (PECSI01, Peccell Technologies, Inc.). The photoelectrochemical characteristics of the QDSSCs were recorded with a potentiostat/galvanostat (PGSTAT 30, Autolab, Eco-Chemie, the Netherlands). Cyclic voltammograms (CVs) were obtained to investigate electrocatalytic abilities of the CEs. Electrochemical impedance spectra (EIS) were obtained by using the above-mentioned potentiostat/galvanostat equipped with an FRA2 module, under a dark condition, at zero bias potential and 10 mV of amplitude over the frequency range of 0.1 Hz–100 kHz. A symmetric sandwich-type cell, consisting of two identical electrodes of area 1 cm^2, a spacer of 25 μm-thick Surlyn® film and a polysulfide elec-

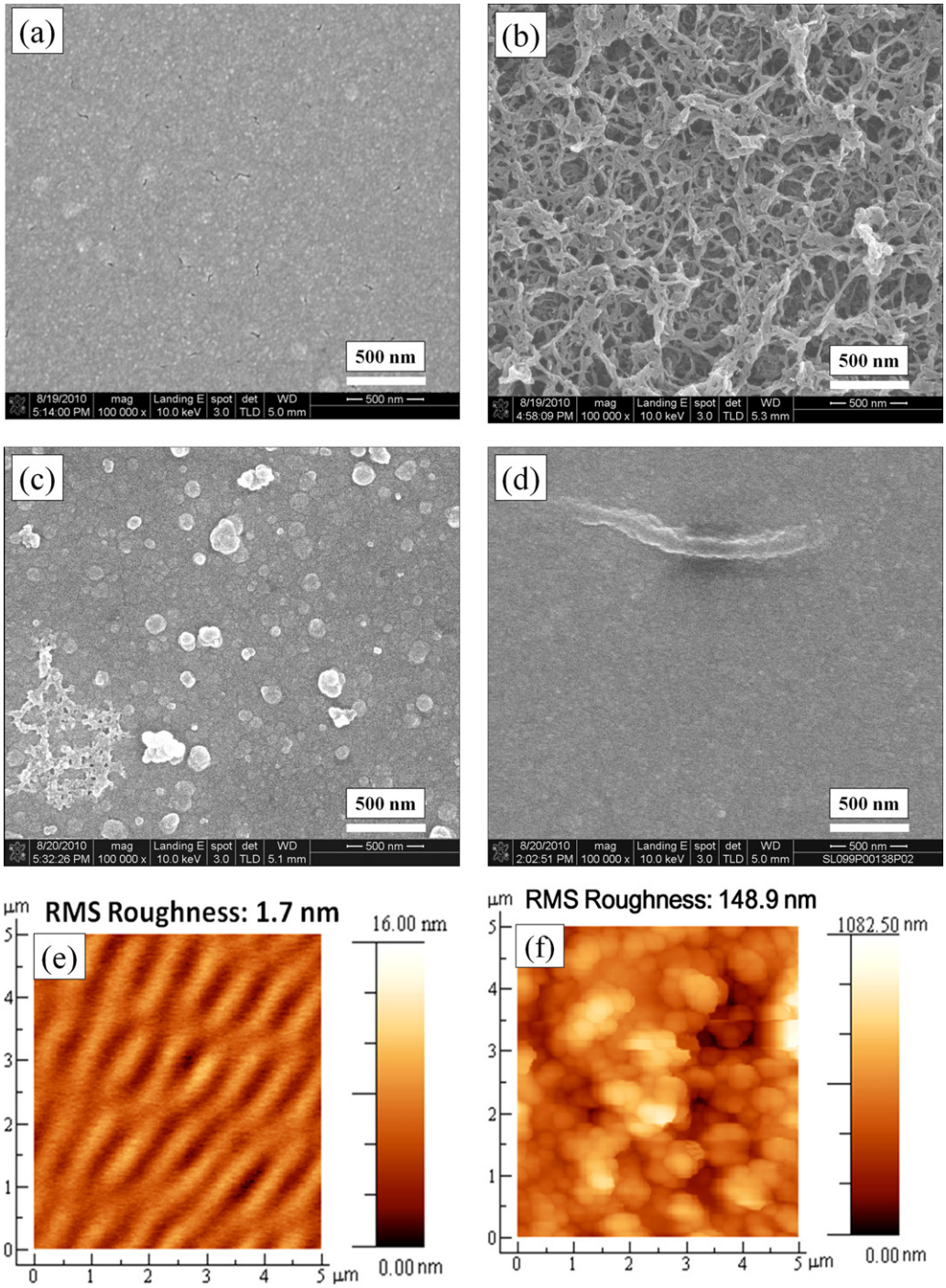

Fig. 1. Top view SEM images of films of (a) sputtered-Au, (b) PEDOT, (c) PT, and (d) PPy, where the conducting polymer films were obtained with 40 mC cm^{-2} as deposition capacity; AFM images (5 μm × 5 μm) of films of (e) sputtered-Au (thickness ~50 nm) and (f) PEDOT (thickness ~200 nm).

trolyte, was used for the EIS measurements. The impedance spectra were analyzed using an equivalent circuit model and evaluated by fitting Nyquist plots to the Z-VIEW software [45].

3. Results and discussion

3.1. Surface morphologies of different conducting polymer films

Fig. 1 shows SEM images of s-Au film and different conducting polymer films (PT, PPy and PEDOT) which were electropolymerized on ITO conducting glasses with a deposition charge capacity of 40 mC cm^{-2}. Fig. 1a shows metallic Au with smooth surface and less porosity, which implies that electrochemical surface area and electrolyte penetration are unfavorable for this kind of structure. Fig. 1b shows the image of PEDOT; the polymer matrix has a regular porous structure with net-like fibers of various dimensions. However, PT and PPy do not exhibit any special matrix structure as can be seen in Fig. 1c and d, respectively. In order to study the surface roughness of films of s-Au (film thickness ~50 nm) and PEDOT (film thickness ~200 nm), high-resolution tapping-mode atomic force microscopy (AFM) was applied, and the images are shown in Fig. 1. It is observed that s-Au film (Fig. 1e) is very smooth (with a root mean square roughness (R_{rms}) of 1.7 nm) and has a regular structure of bending sticks with a few gaps among

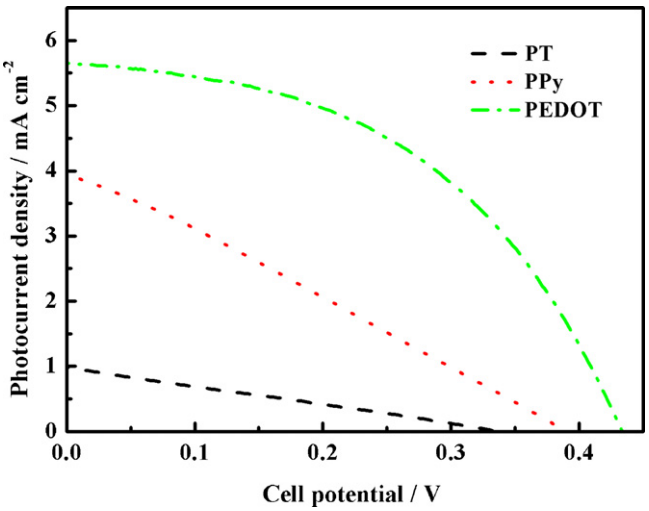

Fig. 2. Photocurrent–potential curves of QDSSCs with CEs of different conducting polymer films, obtained at the constant deposition capacity of 40 mC cm^{-2}.

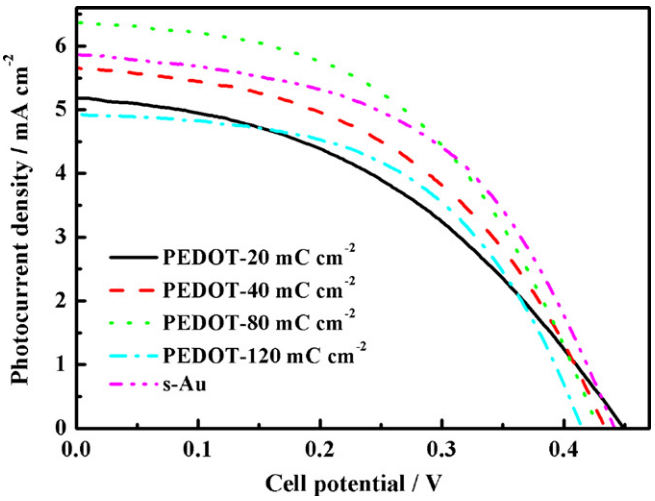

Fig. 4. Photocurrent–potential curves of the QDSSCs with s-Au-CE and PEDOT-CEs, in which the PEDOT films were deposited at different deposition capacities.

them. The morphology of the PEDOT film (Fig. 1f) shows huge three dimensional clusters of sub-microparticles of PEDOT with micropores adjacent to the clusters. The R_{rms} of the PEDOT film, as expected, is of 2 orders higher than that of s-Au film (with the R_{rms} of 148.9 nm); these values can be noted in Fig. 1e and f, respectively. These results imply that the charge-transfer resistance at the electrode/electrolyte interface would be lower in the case of PEDOT-CE, because this CE would have more electrocatalytic active sites for the reaction of polysulfide (S_x^{2-}/S^{2-}) redox couple in the electrolyte [46].

3.2. Photovoltaic performance of QDSSCs with different conducting polymer-based counter electrodes

In order to determine the best CP-based CE for the QDSSCs, different CP-based CEs were employed to assemble different QDSSCs. The photocurrent–potential characteristics of the QDSSCs with different CP-based CEs, obtained at the constant deposition capacity of 40 mC cm^{-2}, are shown in Fig. 2, and the corresponding photovoltaic parameters are summarized in Table 1. It is clear from the table that the cell efficiency (η) is far higher for the QDSSC with PEDOT-CE (1.16%), compared to those with PT-CE (0.09%) and PPy-CE (0.41%). Higher efficiency of the cell with the PEDOT-based CE is due to its higher short-circuit current density (j_{SC}), open-circuit voltage (ΔV_{OC}) and fill factor (*FF*), with reference to these parameters of the cells with PT-CE and PPy-CE. SEM image (Fig. 1) shows that the PEDOT matrix has much higher porosity and surface roughness among the polymers; this is understood to be the reason for PEDOT to facilitate the penetration of electrolyte into the film and to enable more electrochemical active site for S_x^{2-}/S^{2-} redox reaction. The inherent nature of porous and net-like structure of PEDOT can facilitate more diffusion paths and electrocatalytic area for S_x^{2-} ions and thereby the reduction of S_x^{2-} ions, which in turn favors higher j_{SC} for the cell with PEDOT, compared to those in the case of the cells with PT-CE and PPy-CE. This phenomenon will be verified in further discussions through electrochemical impedance spectroscopy (EIS).

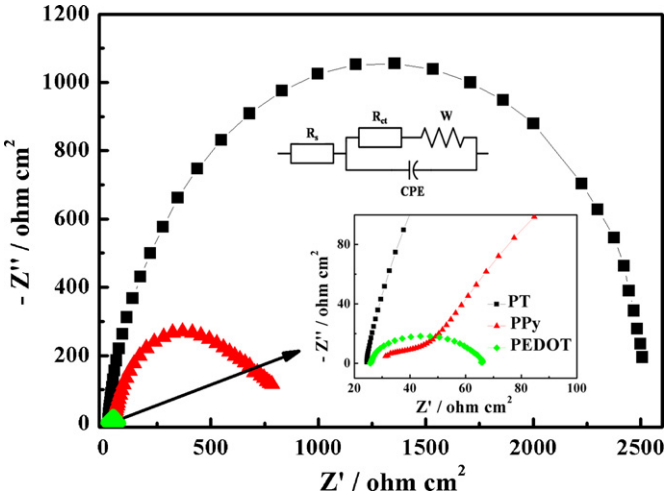

Fig. 3. Nyquist plots of symmetric sandwich-type cells with identical electrodes of different conducting polymer films, measured at zero bias potential; the inset represents the magnified version of the plots in the high frequency range; the equivalent circuit is also included in the figure for fitting the EIS.

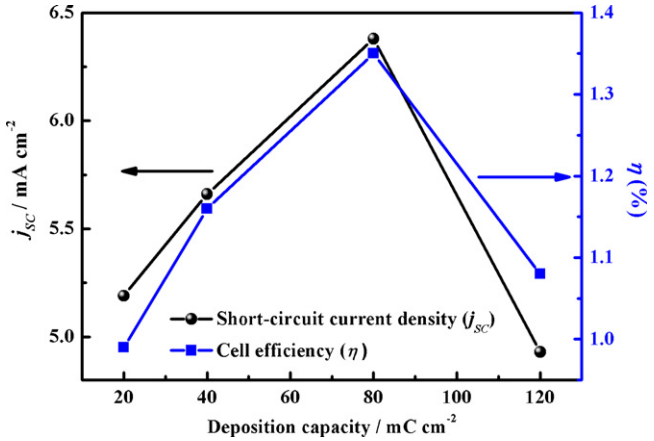

Fig. 5. Behaviors of η and j_{SC} of the QDSSCs with PEDOT-CEs, each as a function of deposition capacity of the PEDOT-film.

Table 1
Photovoltaic parameters of QDSSCs with CEs of different conducting polymer films, obtained at the constant deposition capacity of 40 mC cm^{-2}, the table also shows the R_{ct} values of the symmetric sandwich-type cells with identical CEs.

Samples	η (%)	ΔV_{OC} (mV)	j_{SC} (mA cm^{-2})	*FF*	R_{ct} (Ω cm^2)
PT	0.09	337	0.99	0.26	1267.5
PPy	0.41	390	3.95	0.27	377.5
PEDOT	1.16	435	5.66	0.47	20.1

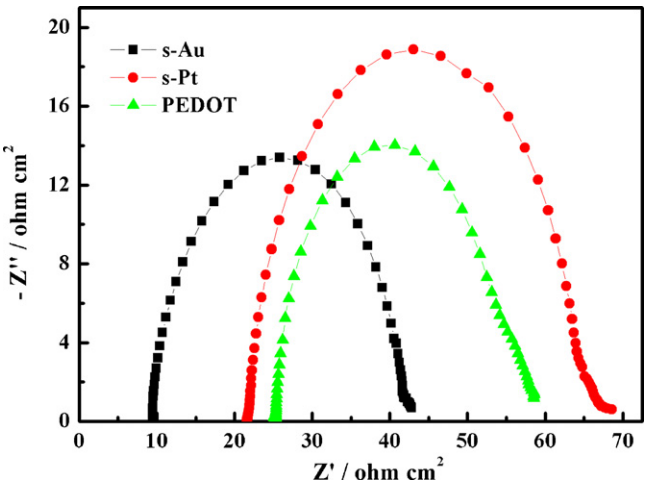

Fig. 6. Nyquist plots of symmetric sandwich-type cells with s-Au electrodes, s-Pt electrodes, and PEDOT electrodes, measured at zero bias potential.

3.3. Electrocatalytic activities of CEs with different conducting polymers for polysulfide ions

In the QDSSCs, electrolyte of S^{2-} plays a key role to keep the regeneration cycle of QDs because its electrons have to be transferred to recover the holes of QDs, which allows the QDs to be regenerated. Therefore, the oxidized species, i.e., S_x^{2-} ions should be continuously reduced at the CE, as per the following reaction [13]:

$$S_x^{2-} + 2e^- \rightarrow S_{x-1}^{2-} + S^{2-} \quad (x = 2\text{–}5) \tag{1}$$

The reduction rate of S_x^{2-} ions at the CE is primarily determined by the electrocatalytic activity and electrochemical active area of the CE. Hence, the charge transfer resistances (R_{ct}) for the reduction of S_x^{2-} ions at different CP-based CEs are investigated by EIS. Fig. 3 shows Nyquist plots of symmetric sandwich-type cells with different CP-based electrodes. In the high frequency region (10^6–10^5 Hz), where the phase is zero, the ohmic series resistance (R_s), including the ITO layer and the CP/electrolyte interface, can be determined. In the middle frequency range (10^5–10 Hz), the impedance associated with the heterogeneous electron transfer at the CE/electrolyte interface can be determined, which consists of the charge transfer resistance (R_{ct}) and the double layer capacitance (CPE). In the low frequency range (10–0.1 Hz), the Warburg diffusion impedance (W) within the electrolyte can be estimated. R_{ct} values of the symmetric sandwich-type cells with PT electrodes, PPy electrodes, and PEDOT electrodes are evaluated by fitting the impedance spectra with the equivalent circuit shown in Fig. 3. The values of R_{ct} are 1267.5, 377.5, and 20.1 Ω cm^2 for the symmetric sandwich-type cells with PT electrodes, PPy electrodes and PEDOT electrodes (40 mC cm^{-2}), respectively. The least R_{ct} value of the cell with PEDOT-CE is owing to its best electrocatalytic activity for S_x^{2-} ions. Less R_{ct} value of the cell with PEDOT-CE renders to it the best photovoltaic performance, particularly in terms of its *FF* (Table 1). These results reveal minimum loss of internal energy at the interface of PEDOT-CE and electrolyte. A reduced R_{ct} in general would lead to a higher *FF*, and thereby to a greater η [47]. Moreover, an increase in *FF* usually renders higher ΔV_{OC} for the pertinent cell. Increasing the *FF* implies that well electron transfer, owing to less R_{ct} value, from the CE to the electrolyte, which causes less overpotential at the CE part in the cell and thereby enables increased ΔV_{OC}.

Table 2
Photovoltaic parameters of the QDSSCs with Au-CE and PEDOT-CEs, in which the PEDOT films were deposited at different deposition capacities; these cell parameters were measured under an illumination of 100 mW cm^{-2}. The table also shows the R_{ct} values of the symmetric sandwich-type cells with identical CEs.

Samples	η (%)	ΔV_{OC} (mV)	j_{SC} (mA cm^{-2})	*FF*	R_{ct} (Ω cm^2)
PEDOT-20 mC cm^{-2}	0.99	450	5.19	0.42	32.6
PEDOT-40 mC cm^{-2}	1.16	435	5.66	0.47	20.1
PEDOT-80 mC cm^{-2}	1.35	429	6.38	0.50	15.4
PEDOT-120 mC cm^{-2}	1.08	415	4.93	0.53	11.2
s-Au	1.33	443	5.87	0.51	16.4

3.4. Influence of deposition capacity of PEDOT on the performance of its QDSSC

Our previous work indicates that PEDOT is a potential candidate as the electrocatalyst of a CE for a QDSSC. The influence of deposition charge on the formation of PEDOT films can be seen in the SEM images (as shown in Appendix). The PEDOT film shows a dense structure at 20 mC cm^{-2} (Fig. A1a), i.e., a thin film of the polymer with fewer pores. The film becomes thicker and the pores are clearly noticeable at the charge capacities of 40 mC cm^{-2} (Fig. A1b). Distinct porous structure appears at 80 mC cm^{-2} (Fig. A1c). However, aggregation of the polymer particles appears with large pores in the film, when the deposition charge capacity is 120 mC cm^{-2} (Fig. A1d). These aggregation and large pores in the film may reduce the electrocatalytic activity of its CE for the reduction of S_x^{2-} ions [48].

The photovoltaic performances of the QDSSCs with s-Au-CE and PEDOT-CEs, obtained at different deposition capacities are shown in Fig. 4, and the corresponding parameters are summarized in Table 2. The QDSSC with PEDOT-CEs obtained at 80 mC cm^{-2} shows a light-to-electricity conversion efficiency of 1.35%, which is slightly better than that of the QDSSC with s-Au-CE (1.33%). This result indicates that PEDOT has the potential to replace Au as the CE material of a QDSSC. A pronounced change is observed for *FF*, which significantly increases from 0.42 to 0.53 with an increase in the deposition capacity from 20 to 120 mC cm^{-2}. We obtained R_{ct} values for these symmetric sandwich-type cells with PEDOT electrodes, obtained at different deposition capacities (EIS not shown); the R_{ct} values are also given in Table 2. A consistent decrease in the R_{ct} values can be noticed in the table with the increase of deposition charge capacity from 20 to 120 mC cm^{-2}. Although higher deposition capacity for PEDOT-CE renders lesser R_{ct} value, the best performance is not observed in the case of the cell using PEDOT-CEs obtained at the highest deposition capacity of 120 mC cm^{-2}. Fig. 5 depicts that the j_{SC} and the η increase from 5.19 to 6.38 mA cm^{-2} and from 0.99 to 1.35%, respectively, when the deposition capacity increases from 20 to 80 mC cm^{-2}. Further increases in the deposition capacity lead to a decrease in the j_{SC} values, which is due to the fact that the aggregation and large pores in the PEDOT-film at these increased deposition capacities reduce the electrochemical active area of the film and thereby its electrocatalytic activity [48]. By optimizing the deposition charge capacity of PEDOT to prepare its CE, a light-to-electricity conversion efficiency of 1.35% could be achieved for its QDSSC, which is slightly better than that obtained for the QDSSC with s-Au as the CE material (1.33%).

3.5. Electrocatalytic properties of Au-CE, Pt-CE, and PEDOT-CE

In a QDSSC, the CE plays an important role to catalyze the reduction of S_x^{2-} ions of the polysulfide electrolyte, which is the most common electrolyte for this type of cell. Although platinum (Pt) is one of the best CE materials for a DSSC, it shows poor performance

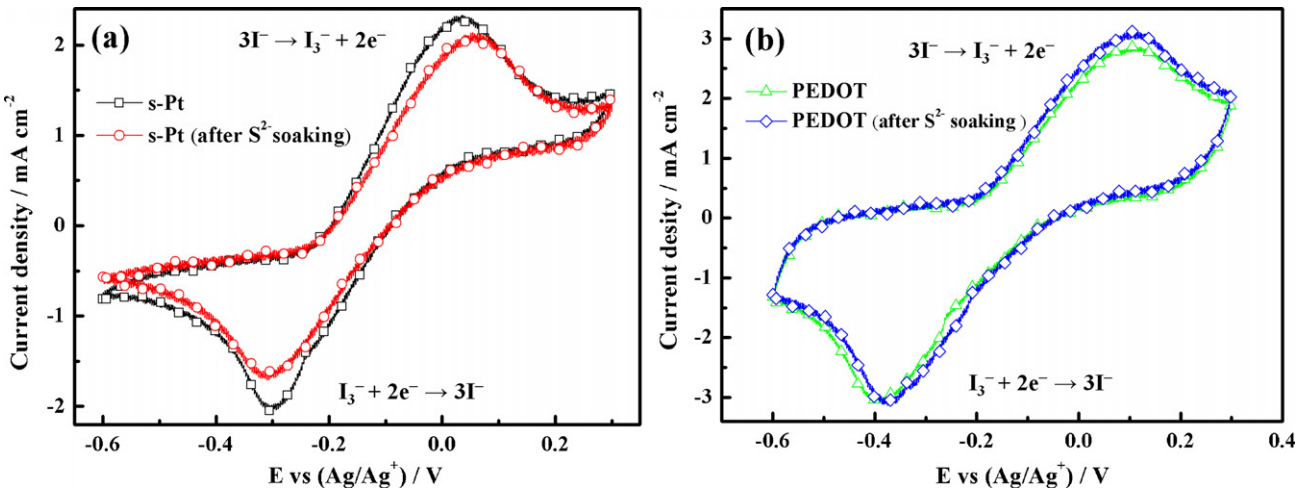

Fig. 7. CVs of (a) s-Pt electrodes with and without pre-soaking in polysulfide electrolyte solution and (b) PEDOT electrodes with and without pre-soaking in polysulfide electrolyte solution, CVs being obtained for I^- and I_3^- species in an electrolyte of 10 mM LiI, 1.0 mM I_2, and 0.1 M $LiClO_4$ in ACN.

in the case of a QDSSC, mainly due to its less electrocatalytic activity, and poor conductivity, as a result of adsorption of sulfide ions on the CE [30]. In order to investigate the electrocatalytic activities of the CEs coated with different materials in a polysulfide electrolyte, EIS and CV were obtained. Fig. 6 shows Nyquist plots of symmetric sandwich-type cells with s-Au electrodes, sputtered-Pt (s-Pt) electrodes, and PEDOT electrodes, with the polysulfide electrolyte. It obviously shows that the s-Pt electrode has the highest R_{ct} value among other electrodes; this is due to its lower electrocatalytic activity in the polysulfide electrolyte, which is consistent with the reported results [32]. Moreover, the PEDOT electrode shows the least R_{ct} value of 15.4 Ω cm^2, which is almost the same as that of an s-Au electrode (16.4 Ω cm^2), owing to its good electrocatalytic activity in the polysulfide electrolyte.

Cyclic voltammograms (CVs) were obtained with three-electrode system to investigate the coverage of sulfide ions on the electrode surface. For this, we soaked an s-Pt electrode in the polysulfide electrolyte solution for 1 h and cleaned its surface with MeOH/water solution (7:3 by volume). Next, we obtained the CV of the electrode in I^-/I_3^- electrolyte solution and then compared its CV with that of the bare electrode, namely, the one without pre-soaking in the polysulfide electrolyte solution. We also obtained the CVs of PEDOT electrode in a similar way in I^-/I_3^- electrolyte solution, i.e., with and without soaking the PEDOT electrodes in the polysulfide electrolyte. The CVs of s-Pt electrodes with and without pre-soaking in polysulfide solution, and CVs of PEDOT electrodes under the same conditions are shown in Fig. 7a and b, respectively. Comparing the CV of the soaked s-Pt electrode with that of the bare s-Pt electrode, it can be seen that the reduction current density decreases in the case of the electrode with soaking; this is because its electrochemical active area was blocked by the adsorption of sulfide ions. However, PEDOT electrode exhibits better performance and stability after its soaking in the polysulfide solution, as can be seen from the CVs in Fig. 7b, in which the currents and charges of CVs are almost the same. The CVs in Fig. 7b reveal that there are poor interactions between the sulfide ions and PEDOT electrode surface.

4. Conclusions

Conducting polymer materials, i.e., polythiophene (PT), polypyrrole (PPy), and poly(3,4-ethylenedioxythiophene) (PEDOT) were used as the catalyst materials of the counter electrodes (CEs) of quantum-dot-sensitized solar cells (QDSSCs). Among the conducting polymers, PEDOT shows a regular porous structure with net-like fibers of various dimensions, while the others do not exhibit any special matrix structure. The QDSSC with PEDOT-CE shows the best efficiency (1.16%, Table 1) with reference to those of the cells with PT-CE (0.09%) and PPy-CE (0.41%). Distinct porous structure appears at the charge capacity of 80 mC cm^{-2} used for the preparation of PEDOT, and the corresponding cell efficiency is maximum at 80 mC cm^{-2} (1.35%). The PEDOT electrode shows the least charge transfer resistance (R_{ct}) value of 15.4 Ω cm^2 at the interface of the counter electrode and the electrolyte, which is almost the same as that of an s-Au electrode (16.4 Ω cm^2). CV data reveal that PEDOT is very suitable for polysulfide electrolyte. Obtainment of slightly higher efficiency for a QDSSC with PEDOT-CE, compared to the efficiency of a QDSSC with Au-based one, implies that PEDOT can replace the expensive Au material in the case of QDSSCs.

Acknowledgements

This work was supported in part by the National Research Council of Taiwan, under grant numbers NSC 98-2120-M-002-003 and NSC 98-3114-E-008-002. Some of the instruments used in this study were made available through the financial support of the Academia Sinica, Taipei, Taiwan, under grant AS-97-TP-A08.

Appendix A. Appendix

See.

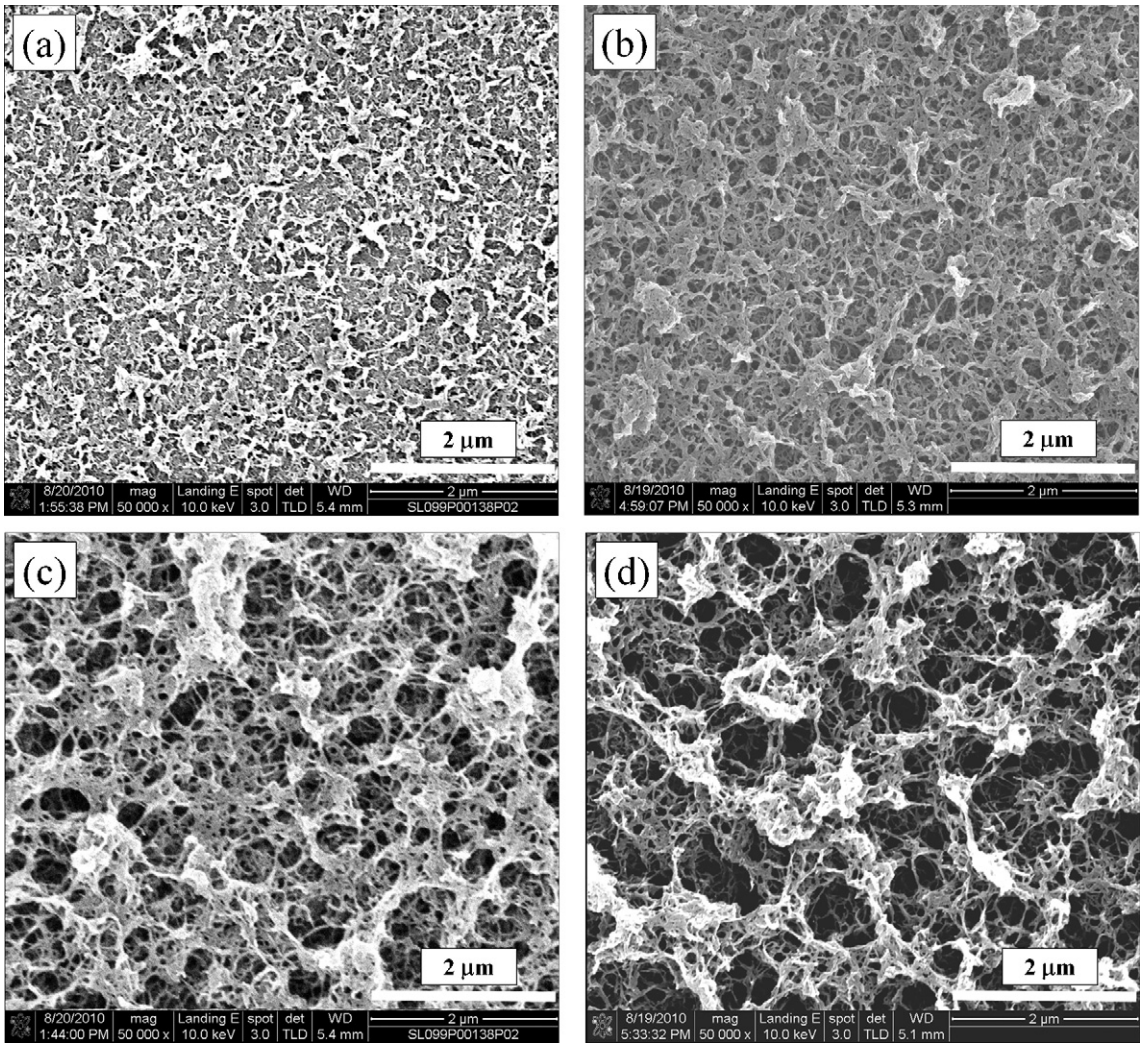

Fig. A1. Top view SEM images of PEDOT films, formed with the deposition capacities of (a) 20, (b) 40, (c) 80, and (d) 120 mC cm^{-2}.

References

[1] B. O'Regan, M. Grätzel, Nature 353 (1991) 737.
[2] M. Grätzel, Inorg. Chem. 44 (2005) 6841.
[3] M. Grätzel, J. Photochem. Photobiol. A: Chem. 164 (2004) 3.
[4] M. Grätzel, Nature 414 (2001) 338.
[5] A. Hagfeldt, M. Grätzel, Acc. Chem. Res. 33 (2000) 269.
[6] A. Hagfeld, M. Grätzel, Chem. Rev. 95 (1995) 49.
[7] C.Y. Chen, S.J. Wu, C.G. Wu, J.G. Chen, K.C. Ho, Angew. Chem. Int. Ed. 45 (2006) 5822.
[8] C.Y. Chen, M. Wang, J.Y. Li, N. Pootrakulchote, L. Alibabaei, C.-h. Ngoc-le, J.D. Decoppet, J.H. Tsai, C. Grätzel, C.G. Wu, S.M. Zakeeruddin, M. Grätzel, ACS Nano 3 (2009) 3103.
[9] D.R. Baker, P.V. Kamat, Adv. Funct. Mater. 19 (2009) 805.
[10] H. Lee, H.C. Leventis, S.J. Moon, P. Chen, S. Ito, S.A. Haque, T. Torres, F. Nüesch, T. Geiger, S.M. Zakeeruddin, M. Grätzel, M.K. Nazeeruddin, Adv. Funct. Mater. 19 (2009) 2735.
[11] W. Lee, S. Min, V. Dhas, S. Ogale, S. Han, Electrochem. Commun. 11 (2009) 103.
[12] M. Shalom, S. Dor, S. Rühle, L. Grinis, A. Zaban, J. Phys. Chem. C 113 (2009) 3895.
[13] Y.L. Lee, C.H. Chang, J. Power Sources 185 (2008) 584.
[14] I. Robel, V. Subramanian, M. Kuno, P.V. Kamat, J. Am. Chem. Soc. 128 (2006) 2385.
[15] L.J. Diguna, Q. Shen, J. Kobayashi, T. Toyoda, Appl. Phys. Lett. 91 (2007) 023116.
[16] S. Giménez, I. Mora-Seró, L. Macor, N. Guijarro, T. Lana-Villarreal, R. Gómez, L.J. Diguna, Q. Shen, T. Toyoda, J. Bisquert, Nanotechnology 20 (2009) 295204.
[17] L.W. Chong, H.T. Chien, Y.L. Lee, J. Power Sources 195 (2010) 5109.
[18] R. Plass, S. Pelet, J. Krueger, M. Grätzel, U. Bach, J. Phys. Chem. B 106 (2002) 7578.
[19] R. Schaller, V. Klimov, Phys. Rev. Lett. 92 (2004) 186601.
[20] A. Zaban, O.I. Mićić, B.A. Gregg, A.J. Nozik, Langmuir 14 (1998) 3153.
[21] P. Yu, K. Zhu, A.G. Norman, S. Ferrere, A.J. Frank, A.J. Nozik, J. Phys. Chem. B 110 (2006) 25451.
[22] G.Y. Lan, Y.W. Lin, Y.F. Huang, H.T. Chang, J. Mater. Chem. 17 (2007) 2661.
[23] S. Cazzanti, S. Caramori, R. Argazzi, C.M. Elliott, C.A. Bignozzi, J. Am. Chem. Soc. 128 (2006) 9996.
[24] S.A. Sapp, C.M. Elliott, C. Contado, S. Caramori, C.A. Bignozzi, J. Am. Chem. Soc. 124 (2002) 11215.
[25] M.C. Hanna, A.J. Nozik, J. Appl. Phys. 100 (2006) 074510.
[26] W. Shockley, H.J. Queisser, J. Appl. Phys. 32 (1961) 510.
[27] A.J. Nozik, R. Memming, J. Phys. Chem. 100 (1996) 13061.
[28] A.J. Nozik, Physica E 14 (2002) 115.
[29] A.J. Nozik, Inorg. Chem. 44 (2005) 6893.
[30] Y.L. Lee, Y.S. Lo, Adv. Funct. Mater. 19 (2009) 604.
[31] Q. Zhang, Y. Zhang, S. Huang, X. Huang, Y. Luo, Q. Meng, D. Li, Electrochem. Commun. 12 (2010) 327.
[32] S.Q. Fan, B. Fang, J.H. Kim, J.J. Kim, J.S. Yu, J. Ko, Appl. Phys. Lett. 96 (2010) 063501.
[33] S.Q. Fan, B. Fang, J.H. Kim, B. Jeong, C. Kim, J.S. Yu, J. Ko, Langmuir 26 (2010) 13644.
[34] M. Deng, Q. Zhang, S. Huang, D. Li, Y. Luo, Q. Shen, T. Toyoda, Q. Meng, Nanoscale Res. Lett. 5 (2010) 986.
[35] Z. Yang, C.Y. Chen, C.W. Liu, H.T. Chang, Chem. Commun. 46 (2010) 5485.
[36] T. Yohannes, O. Inganas, Sol. Energy Mater. Sol. Cells 51 (1998) 193.
[37] Y. Saito, W. Kubo, T. Kitamura, Y. Wada, S. Yanagida, J. Photochem. Photobiol. A: Chem. 164 (2004) 153.
[38] S. Biallozor, A. Kupniewska, Electrochem. Commun. 2 (2000) 480.
[39] S. Ahmad, J.H. Yum, Z. Xianxi, M. Grätzel, H.J. Butt, M.K. Nazeeruddin, J. Mater. Chem. 20 (2010) 1654.
[40] J. Wu, Q. Li, L. Fan, Z. Lan, P. Li, J. Lin, S. Hao, J. Power Sources 181 (2008) 172.
[41] S. Ahmad, J.H. Yum, H.J. Butt, M.K. Nazeeruddin, M. Grätzel, ChemPhysChem 11 (2010) 2814.

[42] M.K. Nazeeruddin, R. Humphry-Baker, P. Liska, M. Grätzel, J. Phys. Chem. B 107 (2003) 8981.
[43] C.J. Barbé, F. Arendse, P. Comte, M. Jirousek, F. Lenzmann, V. Shklover, M. Grätzel, J. Am. Ceram. Soc. 80 (1997) 3157.
[44] C.Y. Huang, Y.C. Hsu, J.G. Chen, V. Suryanarayanan, K.M. Lee, K.C. Ho, Sol. Energy Mater. Sol. Cells 90 (2006) 2391.
[45] A. Hauch, A. Georg, Electrochim. Acta 46 (2001) 3457.
[46] J.G. Chen, H.Y. Wei, K.C. Ho, Sol. Energy Mater. Sol. Cells 91 (2007) 1472.
[47] X. Fang, T. Ma, G. Guan, M. Akiyama, T. Kida, E. Abe, J. Electroanal. Chem. 570 (2004) 257.
[48] K.M. Lee, P.Y. Chen, C.Y. Hsu, J.H. Huang, W.H. Ho, H.C. Chen, K.C. Ho, J. Power Sources 188 (2009) 313.
[49] S.C. Lin, Y.L. Lee, C.H. Chang, Y.J. Shen, Y.M. Yang, Appl. Phys. Lett. 90 (2007) 143517.